Soft Matter

Accepted Manuscript

ROYAL SOCIETY OF CHEMISTRY

www.rsc.org/softmatter

Journal Name

RSCPublishing

ARTICLE

Structure rearrangement in the aqueous solution of surface active ionic liquid 1-butyl-3-methylimidazolium bis(2-ethylhexyl) sulfosuccinate

Cite this: DOI: 10.1039/xoxxoooooox

Tianxiang Yin,[a,†] Jiequn Wu,[a,†] Shuzhen Wang,[a] and Weiguo Shen[a,b,*]

Received ooth January 2012,
Accepted ooth January 2012

DOI: 10.1039/xoxxoooooox

www.rsc.org/

The aggregation behaviors of surface active ionic liquid 1-butyl-3-methylimidazolium bis(2-ethylhexyl) sulfosuccinate in aqueous solutions were investigated by conductometry, densimetry, fluorimetry, ^{1}H nuclear magnetic resonance (^{1}HNMR) spectroscopy, dynamic light scattering (DLS), and transmission electron microscopy (TEM), which confirmed two distinguished critical concentrations. The first critical concentration was believed to be the critical aggregation concentration (CAC), where two different types of aggregates were formed, namely, micelles with size of 10 nm and vesicles with size of 100 nm. The second critical concentration at two-fold CAC was suggested to be resulted from the insert of the imidazolium cations into aggregates.

1. Introduction

Ionic liquids (ILs), usually defined as liquid salts below 100℃, are considered as good candidates for green solvents because of their unique properties such as wide liquid state ranges, negligible vapor pressures, favourable solvation behaviors etc.[1] Some types of ILs with long alkyl chains can self-assemble to form micelles or vesicles.[2] Eastoe et al.[3] reported the aggregation behavior of a new type catanionic surface active ionic liquid comprised of quaternary ammonium or 1-butyl-3-methylimidazolium (C_4mim) as a cation and dodecylsulfate (DS) or bis(2-ethylhexyl) sulfosuccinate (AOT), or tri(2-ethylhexyl) sulfosuccinate (TC) as an anion. Kumar et al.[4] investigated the aggregation behaviors of AOT-based surface active ionic liquids (SAILs) with different cations like 1-butyl-3-methylimidazolium, proliniumisopropylester, cholinium, and guanidinium and found the existence of an unusual second critical concentration at about two-fold value of the usual aggregate formation concentration (CAC) in 1-butyl-3-methylimidazolium bis(2-ethylhexyl) sulfosuccinate (C_4mim-AOT) aqueous solution from the isothermal titration calorimetry (ITC) and ^{1}H nuclear magnetic resonance (^{1}H NMR) measurements. However, the presence of the second critical concentration after critical micellization concentration (CMC) has also been observed for sodium bis(2-ethylhexyl) sulfosuccinate (Na-AOT) by means of densimetry[5] and ITC[6] and was denoted as the critical vesicle concentration (CVC). After careful comparison, it is worth to notice that the ITC measurement on the C_4mim-AOT aqueous solutions reported by Kumar et al.[4] showed an exothermic transition process at the concentration of two-fold CAC, where the absolute value of the enthalpy was nearly the same as that in the aggregation formation process around the first critical aggregation concentration;[4] while for Na-AOT, the absolute value of enthalpy for the formation of vesicle at CVC was much less than that for the micellization.[6] Thus, different mechanisms may exist in these two systems at the second critical concentration. Kumar et. al[4] proposed that the first CAC was denoted as the formation of vesicles while the incorporation of the imidazolium cation into the vesicle bilayer without significantly changes of the vesicle size and structure might result in the second transition at two-fold CAC in C_4mim-AOT system, which was similar as that observed in the aqueous solution of 1-butyl-3-methylimidazolium octylsulfate.[7] This proposition was thought to be supported by measurements of the dynamic light scattering (DLS) and the transmission electron microscopy (TEM),[4] which revealed that the formed aggregates had only vesicle sizes from the first transition concentration to the concentration above the second transition point; although very recently Cheng et al.[8] observed bimodal distribution of aggregate size at about 10 nm and 100 nm for the same system. However, above observations are unable to convincingly confirm the proposed mechanisms of two phase transitions, especially the unusual second phase transition, in C_4mim-AOT aqueous solution. Therefore, more techniques and deeper analysis are highly required to further testify this interesting proposed mechanism, including to clarify whether such transitions are similar to those observed in Na-AOT system or not. Because penetration of the C_4mim counterion into the interface layers of aggregates may change the conductivity of the system and the volumetric properties and

the microenvironments of the aggregates, it is expected to be detected by measurements of conductivity, density, fluorescence spectra, and ^{1}H NMR. In this work, we carry out these measurements to explore the mechanism of the second phase transition for the C_4mim-AOT aqueous solution. The negative stained TEM and DLS measurements are also taken to clarify the coexistence of micelles and vesicles in the system and the results are compared with those of Na-AOT system to further testify the Kumar's proposition.

2. Experimental

2.1 Materials

C_4mim-AOT was synthesized by reaction of equi-molar of C_4mimBr and Na-AOT (both supplied by Aladdin (Shanghai, China), >98% mass fraction).[3a,4,8] The mixture was stirred in dichloromethane at room temperature overnight. The precipitation was removed by filter and the dichloromethane layer was washed by water for several times to remove the bromide ion. Thereafter, the solvent was rotary evaporated to get the product, which was further dried under vacuum for 2-3 days before use. The chemical structure of C_4mim-AOT is shown in Scheme 1.

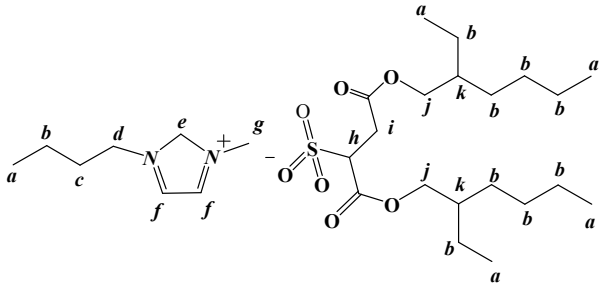

Scheme 1 The chemical structure of C_4mim-AOT

^{1}H NMR (400MHz, in D_2O) was used to characterize the product and the chemical shifts of each proton are as follows: δ=8.65 (e, 1H), 7.36-7.42 (f, 2H), 3.76-4.26 (d,g,j,h, 10H), 2.92-3.20 (i, 2H), 1.77 (c, 2H), 1.53 (k, 2H), 1.05-1.42 (b, 18H), 0.68-0.94 (a, 15H). Moreover, the elementary analysis gave (%, in mass): C, 59.34; N, 4.97; H, 9.58, showing good agreements with theoretical ones, i.e. C, 59.97; N, 5.00; H, 9.35.

The pyrene (≥99% mass fraction) used in the fluorescence measurements was purchased from Sigma-Aldrich Chemical Co. and no further purification was performed before experiments. D_2O (≥99.9% mass fraction) was supplied by Aladdin (Shanghai, China). Double-distilled water was used in the preparations of all aqueous solutions.

2.2 Methods

Conductivity measurement: Conductivity measurements were performed with a digital conduct meter supplied by Leici Co. (Shanghai, China) with a titration method. The conduct meter was initially calibrated by standard KCl solution with concentration of 0.01 mol·L^{-1}. A certain amount of water was transferred into a cell, which was placed in a water bath with temperature being controlled within ±0.1 K. The concentrated surfactant solution was prepared and titrated into the cell by a microsyringe. The cell was shaken after each titration and kept undisturbed to reach thermal equilibrium before measurement. The experiments were conducted at 298.15±0.1 K.

Density measurement: The densities of the aqueous solutions of C_4mim-AOT with various concentrations of the surfactant were determined with a U-tube density meter (Anton Paar, Model DMA 5000M) by measuring the oscillation periods.[5] The density meter was calibrated with both dry air and distilled water at ambient pressure before each measurement. The reproducibility and the accuracy for the measurement of the density, and the precision for the measurement of temperature were claimed to be ±1.10^{-6} g.cm^{-3}, ±5.10^{-6} g.cm^{-3}, and ±0.001 K by the manufacturer, respectively. A series of C_4mim-AOT aqueous solutions with different concentrations were prepared by weighting with a relative uncertainty of the concentration being 0.05%. All the density measurements were conducted at 298.15 K.

Fluorescence measurements: The steady-state fluorescence measurements were conducted for a series of C_4mim-AOT aqueous solutions with various concentrations of the surfactant using a fluorimeter supplied by Edinburgh Instrument (Model FLS 920), equipped with a 450 mW Xe arc lamp as a light source and a PMT detector (R928P Hamamatsu). The sample was filled in a quartz cuvette with a path length of 1 cm. The temperature in the cuvette was controlled by a water-circulating bath with the stability of ±0.1 K. Pyrene was used as the probe to investigate the micropolarity of the system characterized by the intensity ratio (I_1/I_3) of the first peak (373nm) to the third peak (383nm) of the emission spectrum. The sample was excited at 335 nm and the emission spectra were scanned from 350 nm to 500 nm with an interval of 1 nm at the temperature T=298.15 ± 0.1 K.

***Dynamic light scattering (DLS)*:** Hydrodynamic radius of the aggregates in C_4mim-AOT aqueous solutions with different surfactant concentrations were measured by dynamic light scattering using the Malvern Zetasizer Nano ZS instrument (Southborough, MA) with a backscattering detector (173°) and a laser of 633 nm wavelength. Measurements were taken in a batch mode at 298.15 K using a quartz cuvette with a path length of 1 cm.

Transmission Electron Microscopy (TEM): The samples for TEM measurements were prepared by a negative stained method using 1% uranyl acetate solution as a stained agent. A drop of solution was placed on a carbon coated cooper grid (300 mesh) and the excess liquid was sucked away by filter paper. The images of samples after drying in room temperature were obtained by the JEM-1400 electron microscope at working voltage of 120kV.

Nuclear magnetic resonance measurements (NMR): ^{1}H NMR spectra of C_4mim-AOT solutions in D_2O were collected by using the Avance spectrometer (400MHz, Bruker).

3. Results and discussions

The plot of conductivity against C_4mim-AOT concentration is shown in Figure 1. Unlike that reported by Kumar et. al.,[4] two distinguished breaking points i.e. the intersections of three linear regions were taken as the critical concentrations and denoted as the critical aggregation concentration (CAC) and C_2, which were determined to be 2.05 ± 0.10 mM and 3.20 ± 0.10 mM, respectively. The CAC value was in good agreement with that determined in the literature by the same method, i.e. 1.9 ± 0.1 mM.[8] The degree of counterion binding β_{CAC} calculated from the slopes before and after CAC was 0.52 ± 0.02. The obtained value of β_{CAC} was larger than that observed in Na-AOT system,[8] which may be attributed to the less solvation ability of large C_4mim cation, hence more cations bound at the interface mainly through the electrostatic interaction. Moreover, due to the weak hydrophobicity of the butyl chain on the cation, some cations may insert into the interface with alkyl chain toward the hydrophobic core through the hydrophobic interaction, which might also result in larger value of β_{CAC} for C_4mim-AOT system. The standard Gibbs free energy of the aggregation was calculated by[9]

$$\Delta G_m = (1+\beta_{CAC})RT\ln X_{CAC} \quad (1)$$

where X_{CAC} is mole fraction of C_4mim-AOT at CAC. The obtained value of ΔG_m was -38.5±0.5 kJ·mol^{-1}. Both β_{CAC} and ΔG_m values are in reasonable agreements with those reported by different research groups.[4,8] The degree of counterion binding β_{C2} after C_2 was also calculated and found to be 0.88 ± 0.02. The increasing value of β_{C2} indicates that more counterions presented at the aggregates' interface after C_2. It is reasonable to propose that significantly more counterions insert into the interface with hydrophobic chains toward the inner core after C_2 to maintain the hydrophility/hydrophobility balance in the system.

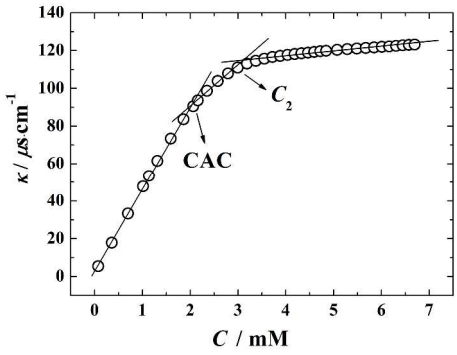

Figure 1 Plot of conductivity against concentration of C_4mim-AOT

The apparent molar volume of C_4mim-AOT V_φ in the C_4mim-AOT aqueous solution is defined as:

$$V_\varphi = \frac{V - n_w V_w}{n_s} \quad (2)$$

where V, V_w, n_w, and n_s are the volume of the solution, the molar volume of water, the molar quantity of water and the molar quantity of surfactant, respectively. The apparent molar volume of C_4mim-AOT can be calculated from the measured densities of C_4mim-AOT aqueous solutions by[10]

$$V_\varphi = \frac{M}{\rho} + \frac{10^6(\rho_0 - \rho)}{m\rho\rho_0} \quad (3)$$

where M, m, ρ_0, and ρ are the molar mass of C_4mim-AOT (g·mol^{-1}), the concentration of C_4mim-AOT in aqueous solutions (mmol·kg^{-1}), the density of water (g·cm^{-3}), and the density of the C_4mim-AOT aqueous solution (g·cm^{-3}), respectively. The calculated values of the apparent molar volume are plotted against the reciprocal of the C_4mim-AOT concentration in Figure 2, where the critical concentrations CAC and C_2 were determined as the intersections of the extrapolations of the slowly changing linear portions and the rapidly changing linear portion of the curve. The values of CAC and C_2 were determined to be 1.88±0.08 mM and 3.13±0.06 mM, which were in well agreement with those in the conductivity measurement.

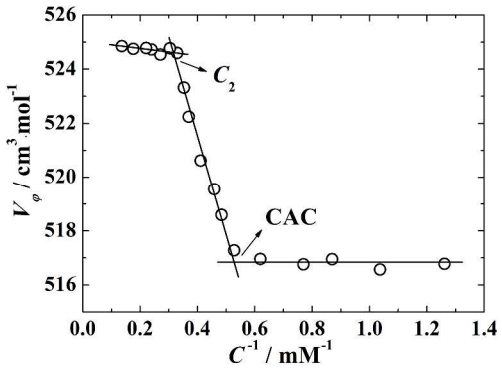

Figure 2 Plot of apparent molar volume of C_4mim-AOT against the reciprocal of C_4mim-AOT concentration

It can be seen from Figure 2 that the apparent molar volume of C_4mim-AOT changes little in the pre-aggregation region and shows significant increase after CAC, which may be attributed to the release of the high order structure water in the "ice-berg" near the hydrophobic tails.[11] The variance of the apparent molar volume of C_4mim-AOT after CAC looks similar to those of Na-AOT system[5] reported by us previously. However, after C_2, the increase rate of the apparent molar volume slows down, but does not level off as we observed for Na-AOT system after CVC.[5] This difference possibly characterizes the different phase transitions, which may be interpreted more detailly as follows. With the hypothesises of the pseudophase equilibrium and the ideal dilute surfactant sulution, the concentration of the monomer surfactant in the continuous phase keeps unchanged and the linear change of the apparent molar volume of the surfactant with the reciprocal of the concentration after CAC is approximately attributed to the change of the amount ratio of the monomer surfactant to the surfactant in the micelle;[5,12] thus the abrupt change of apparent molar volume at the second critical concentration might mainly be attributed to the structure change of the aggregates. In Na-AOT system, the closely packed vesicle structure after CVC significantly reduces the increase of the apparent molar volume of Na-AOT, while in

C_4mim-AOT system, insert of the cations into the aggregates loosens the original aggregates' structure.

Dynamic light scattering measurements were performed at the concentrations of C_4mim-AOT at 2.5mM (>CAC) and 5mM (>C_2), which are shown in Figure 3. Unlike that reported by Kumar et. al.,[4] two different types of aggregates were observed with sizes being about 10 nm and 100 nm, respectively. The same bimodal size distribution was observed by Cheng.[8] These results indicate the coexistence of small micelles and large vesicles before C_2, which further support that the second critical concentration in C_4mim-AOT system doesn't characterize the vesicle formation. To further visualize the actual morphology of vesicles, the negative stained TEM technique[13] was used to obtain the images of the aggregates in the C_4mim-AOT aqueous solutions at the concentrations of 2.5 mM and 5 mM, which are shown in Figure 4. The large size vesicles were observable in both concentrations and the sizes were in good agreements with those determined by DLS. The same TEM technique was used to detect the vesicle formation before and after the second critical concentration (CVC) for Na-AOT system, however the vesicles were only observed after CVC.[6] Therefore, it suggests that different phase transitions are presented in C_4mim-AOT and Na-AOT systems at the second critical concentrations.

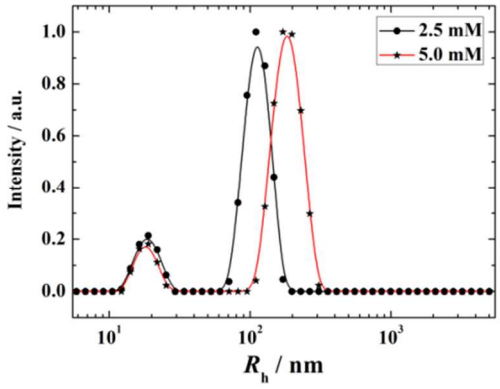

Figure 3 Size distributions of C_4mim-AOT aqueous solutions

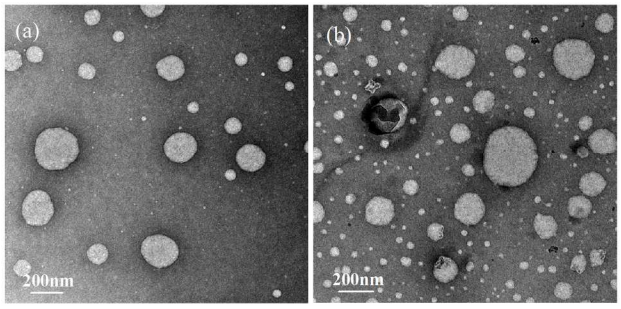

Figure 4 TEM images of C_4mim-AOT aqueous solutions with concentrations being (*a*) 2.5mM and (*b*) 5mM.

In order to gain more microscopic information of the aggregates, steady-state fluorescence measurements were conducted with pyrene as a probe. As shown in Figure 5a, the value of I_1/I_3 keeps almost unchanged first; after a certain concentration of C_4mim-AOT, it sharply decreases with the increase of the concentration of C_4mim-AOT and then keeps almost constant again. However, further addition of C_4mim-AOT results in the increase of I_1/I_3, and finally it levels off once again. The critical concentrations CAC and C_2 were determined as the intersections of the extrapolations of the almost level linear portions and the lineally rapidly changing portions of the curve as illustrated in Figure 5a.[14] The values of critical concentrations of CAC and C_2 were determined to be 1.7±0.10 mM and 3.6 ±0.1 mM, respectively; which showed reasonable agreements with those determined by measurements of the conductivity and the apparent molar volume.

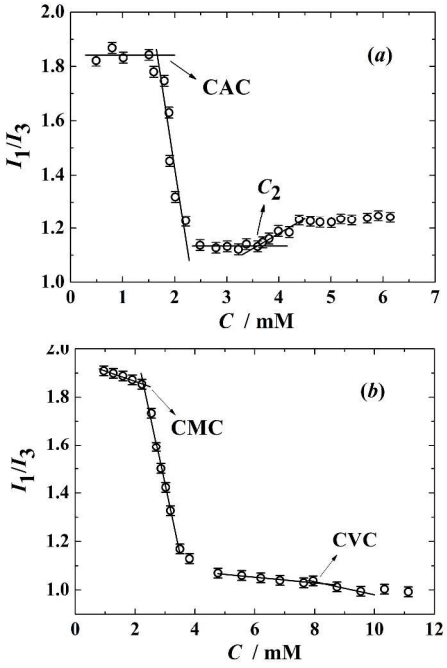

Figure 5 Plot of I_1/I_3 values against surfactant concentrations for (*a*) C_4mim-AOT and (*b*) Na-AOT. The dots are experimental data, while the lines are linear fitting results.

For comparison, the values of I_1/I_3 of Na-AOT aqueous solutions were also measured and are shown in Figure 5b. The CMC and CVC values determined by the same way described above were 2.30±0.09 mM and 8.10±0.10 mM, respectively, which coincide well with the reported ones.[5,6,15] The decrease of I_1/I_3 after CMC was attributed to the migration of pyrene molecules to the non-polar palisade layer of aggregates, while slightly further decrease of the I_1/I_3 value was observed due to more compact structure of vesicles formed after CVC.

As shown in Figure 5a, contrary to the Na-AOT aqueous solution, the I_1/I_3 value increases with the surfactant concentration after C_2 for C_4mim-AOT system, suggesting the different mechanism from that in Na-AOT system. It may be interpreted by that the insert of the hydrophobic tails of imidazolium cations into the aggregates after C_2 loosens the structure of the aggregates and allows more polar heads of imidazolium cations and water to penetrate into the palisade layer where pyrene located, hence increases the polarity in the palisade layer and the measured value of I_1/I_3.

The above observed experimental results may be explained by the mechanism as illustrated in Scheme 2. When the surfactant concentration is higher than CAC, the aggregates with two different sizes are formed in the system. The release of structured water nearby the hydrophobic tails during the aggregate formation increases the apparent molar volume of C_4mim-AOT. The binding of imidazolium cations on the interface of aggregates lowers the increase rate of conductivity. Meanwhile, the migration of pyrene into the hydrophobic region of aggregates reduces the I_1/I_3 value. With the further increase of surfactant concentration up to C_2, much more imidazolium cations insert into the aggregates' interface through the hydrophobic interaction and loosen the aggregates' structure, which results in the further decrease of the slope of the linear plot of the conductivity *vs.* surfactant concentration and the increase of the polarity of palisade layer and hence the increase of I_1/I_3 value. Moreover, loosening the aggregates' structure due to the penetration of the imidazolium cations causes a continuous slow increase of the apparent molar volume of the surfactant with the surfactant concentration after C_2 rather than leveling off as it is in Na-AOT vesicles after CVC.

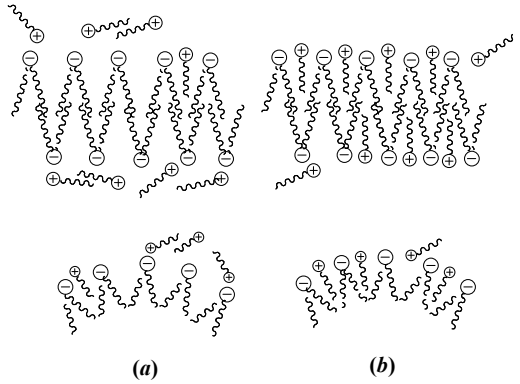

Scheme 2 The aggregates' structure after (a) CAC and (b) C_2

Furthermore, the measurements of chemical shifts of protons on surfactants may provide us direct information of the structure change of the aggregates since they are sensitive to the local micro-environment.[16] Kumar et. al.[4] have measured the chemical shifts of proton on the imidazolium cation, however the measured results were only used to confirm the existence of the second critical concentration observed by ITC and no further analysis and discussion were presented. Here we report the measurements of the chemical shifts both of protons *e* and *k* (see scheme 1) on C_4mim cation and AOT anion at various surfactant concentrations, which are plotted in Figures 6a and 6b respectively.

As shown in Figure 6a, the chemical shift of proton *e* in the imidazolium cation shows down-field shift after CAC (about 1.8 mM), which may be attributed to that part of the imidazolium cations bind to the interface of aggregates after CAC and reduce their average hydrophility as compared in the bulk solution. The much sharper down-field shift after C_2 may indicate that the proton *e* locates in more hydrophobic environment as the penetration of imidazolium cations into the

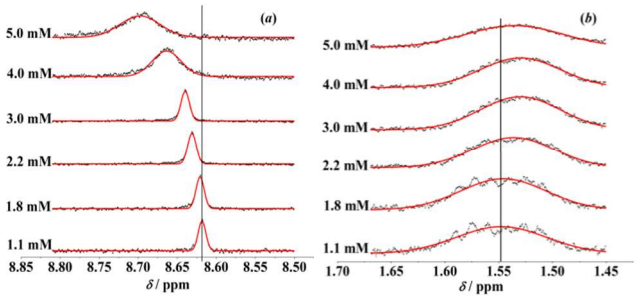

Figure 6 Partial ^{1}H NMR spectra of (*a*) proton *e* in the C_4mim cation and (*b*) proton *k* in the AOT anion at various concentrations

aggregates. Figure 6b provides new phase transition information through the chemical shift of proton *k* in alkyl chain of bis(2-ethylhexyl) sulfosuccinate anion. The chemical shift of proton *k* shows obvious up-field shift after CAC, while a little down-field shift after C_2 is displayed. Generally, the decrease of the polarity of the microenvironment where alkyl chain is located would cause downfield shift of the proton's chemical shift.[17] However, the conformational change of alkyl chain from *trans* to *gauche* may cause up-field shift,[7,16f] moreover, the shielding effect from the imidazolium ring located on the interface may also cause the up-field shift of the protons on AOT alkyl chains.[18] Therefore, the conformational change and the effect from the imidazolium ring possibly dominate the change of the chemical shift of proton *k* in the aggregation process after CAC. However, after C_2, imidazolium cations insert into the aggregates core in the structure transition and increase the hydrophobicity of the micro-environment significantly, which results in the dominance of the hydrophobicity effect on the change of the chemical shift of proton *k*. Above two ^{1}HNMR experimental results supported two different mechanisms of phase transitions at CAC and C_2.

4. Conclusions

To sum up, the aggregation behavior of surface active ionic liquid 1-butyl-3-methylimidazolium bis(2-ethylhexyl) sulfosuccinate in aqueous solution was investigated by conductometry, densimetry, fluorimetry, DLS, ^{1}HNMR, and negative-stained TEM. Two different types of aggregates were likely formed, namely, micelles with size of 10 nm and vesicles with size of 100 nm after CAC. Moreover, a second critical concentration at two-fold CAC was observed and it was suggested to be resulted from the insert of the imidazolium cations into the aggregates.

Acknowledgements

This work was supported by the National Natural Science Foundation of China (Projects 21173080, 21373085 and 21303055) and the Fundamental Research Funds for the Central Universities (No. WJ1516001).

Notes and references

[a] School of Chemistry and Molecular Engineering, East China University of Science and Technology, Shanghai 200237, China.

[b] Department of Chemistry, Lanzhou University, Lanzhou, Gansu 730000, China.
* Corresponding author: Tel.: +86 21 64250804. Fax: +86 21 64250804. E-mail: shenwg@ecust.edu.cn
† Tianxiang Yin and Jiequn Wu contributed equally as the first authors.

1 J. Dupont, *Acc. Chem. Res*., 2011, **44**, 1223.
2 (a) Z. G. Asadov, G. A. Akhmedova, A. D. Aga-Zadeh, Sh. M. Narbalieva, A. M. Bagirova, and R. A. Ragimov, *Russ. J. Gen. Chem.*, 2012, **82**, 1916; (b) C. C. Villa, F. Moyano, M. Ceolin, J. J. Silber, R. D. Falcone, and N. M. Correa, *Chem. Eur. J*., 2012, **18**, 15598; (c) K. S. Rao, T. J. Trivedi, and A. Kumar, *J. Phys. Chem. B*, 2012, **116**, 14363; (d) H. Y. Wang, L. M. Zhang, J. J. Wang, Z. Y. Li, and S. J. Zhang, *Chem. Comm*., 2013, **49**, 5222.
3 (a) P. Brown, C. P. Butts, J. Eastoe, D. Fermin, I. Grillo, H. C. Lee, D. Parker, D. Plana, and R. M. Richardson, *Langmuir*, 2012, **28**, 2502; (b) P. Brown, C. P. Butts, J. Eastoe, I. Grillo, C. James, and A. Khan, *J. Colloid Interface Sci*, 2013, **395**, 185.
4 K. S. Rao, P. S. Gehlot, T. J. Trivedi, and A. Kumar, *J. Colloid Interface Sci.*, 2014, **428**, 267.
5 Z. G. Zhang, H. H. Wang, P. Z. Zheng, and W. G. Shen, *Colloids Surf. A*, 2013, **421**, 193.
6 Y. R. Fan, Y. J. Li, G. C. Yuan, Y. L. Wang, J. B. Wang, C. C. Han, and H. K. Yan, *Langmuir*, 2005, **21**, 3814.
7 T. Singh, M. Drechsler, A. H. E. Mueller, I. Mukhopadhyay, and A. Kumar, *Phys. Chem. Chem. Phys.*, 2010, **12**, 11728.
8 N. Cheng, X. Y. Ma, X. Sheng, T. Wang, R. Wang, J. J. Jiao, and L. Yu, *Colloids Surf. A*, 2014, **453**, 53.
9 R. Zana, *Langmuir*, 1996, **12**, 1208.
10 C. F. Du, H. H. Wang, T. X. Yin, and W. G. Shen, *J. Chem. Thermodyn.*, 2013, **64**, 226.
11 (a) Z. G. Zhang, H. H. Wang, and W. G. Shen, *J. Chem. Eng. Data*, 2013, **58**, 2326; (b) P. A. Bhat, F. A. Sheikh, and H. I. Tantry, *J. Chem. Eng. Data*, 2014, **59**, 2013.
12 J. B. Rosenbolm, *Colloid Polym. Sci.*, 1981, **259**, 1116.
13 (a) Z. L. Huang, J. Y. Hong, C. H. Chang, and Y. M. Yang, *Langmuir*, 2010, **26**, 2374; (b) A. Roy, M. Maiti, and S. Roy, *Langmuir*, 2012, **28**, 12696.
14 (a) J. H. Mathias, M. J. Rosen, and L. Davenport, *Langmuir*, 2001, **17**, 6148; (b) B. L. Peng, Y. L. Hao, H. M. Kang, X. Han, C. J. Peng, and H. L. Liu, *Carbohydr. Res.*, 2010, **345**, 101; (c) M. R. Nabid, S. J. T. Rezaei, R. Sedghi, H. Niknejad, A. A. Entezami, H. A. Oskooie, and M. M. Heravi, *Polymer*, 2011, **52**, 2799; (d) H. Xing, P. Yan, and J. X. Xiao, *Soft Matter*, 2013, **9**, 1164.
15 P. Z. Zheng, X. Q. An, and W. G. Shen, *J. Phys. Chem. B*, 2009, **113**, 13556.
16 (a) M. Figueira-Gonzalez, V. Francisco, L. Garcia-Rio, E. F. Marques, M. Parajo, and P. Rodriguez-Dafonte, *J. Phys. Chem. B*, 2013, **117**, 2926; (b) J. H. Lin, W. S. Chen, and S. S. Hou, *J. Phys. Chem. B*, 2013, **117**, 12076; (c) M. E. Amato, E. Caponetti, D. C. Martino, and L. Pedone, *J. Phys. Chem. B*, 2003, **107**, 10048; (d) P. Taboada, D. Attwood, J. M. Ruso, F. Sarmiento, and V. Mosquera, *Langmuir*, 1999, **15**, 2022; (e) X. H. Cui, S. Z. Mao, M. L. Liu, H. Z. Yuan, and Y. R. Du, *Langmuir*, 2008, **24**, 10771; (f) T. Singh, and A. Kumar, *J. Phys. Chem. B*, 2007, **111**, 7843.
17 (a) U. R. K. Rao, C. Manohar, B. S. Valaulikar, and R. M. Iyer, *J. Phys. Chem.*, 1987, **91**, 3286; (b) E. B. Tada, L. P. Novaki, and O. A. El Seoud, *Langmuir*, 2001, **17**, 652; (c) L. J. Shi, N. Li, H. Yan, Y. A. Gao, and L. Q. Zheng, *Langmuir*, 2011, **27**, 1618.
18 (a) L. T. Okano, O. A. El Seoud, and T. K. Halstead, *Colloid Polym. Sci.*, 1997, **275**, 138; (b) S. Shimizu, and O. A. El Seoud, *Langmuir*, 2003, **19**, 238; (c) B. Dong, Y. A. Gao, Y. J. Su, L. Q. Zheng, J. K. Xu, and T. Inoue, *J. Phys. Chem. B*, 2010, **114**, 340; (d) L. J. Shi, and L. Q. Zheng, *J. Phys. Chem. B*, 2012, **116**, 2162.

